UNIVERSITY OF ARIZONA
STUDENT SATELLITE PROJECT

Technical Note

Doc. no.: GNC-005

Revision no.: 1.0

Status: Draft

Subject: Reaction Wheel Overview **Date:** May 7, 1998

Written by: Barry Goeree, Jerry Morales, and Greg Chatel

Reviewed by: Dr. Fasse

Revision history:

Revision 1.0: Initial Draft

---

1. Document Overview

This report describes the design of low cost reaction wheels for use on UASat. In essence, a reaction wheel is an electric motor with a heavy disk attached to its axis. By applying a current to the motor, a torque can be generated to change the angular velocity of the disk. According to Newton's third law, a reaction torque with the same magnitude and opposite sign will then act on the satellite. The control system uses this torque to reorient the spacecraft when a vehicle pointing error (deviation from the desired attitude) is detected by the GNC sensors. Figures 1-1 and 1-2 show a typical reaction wheel.

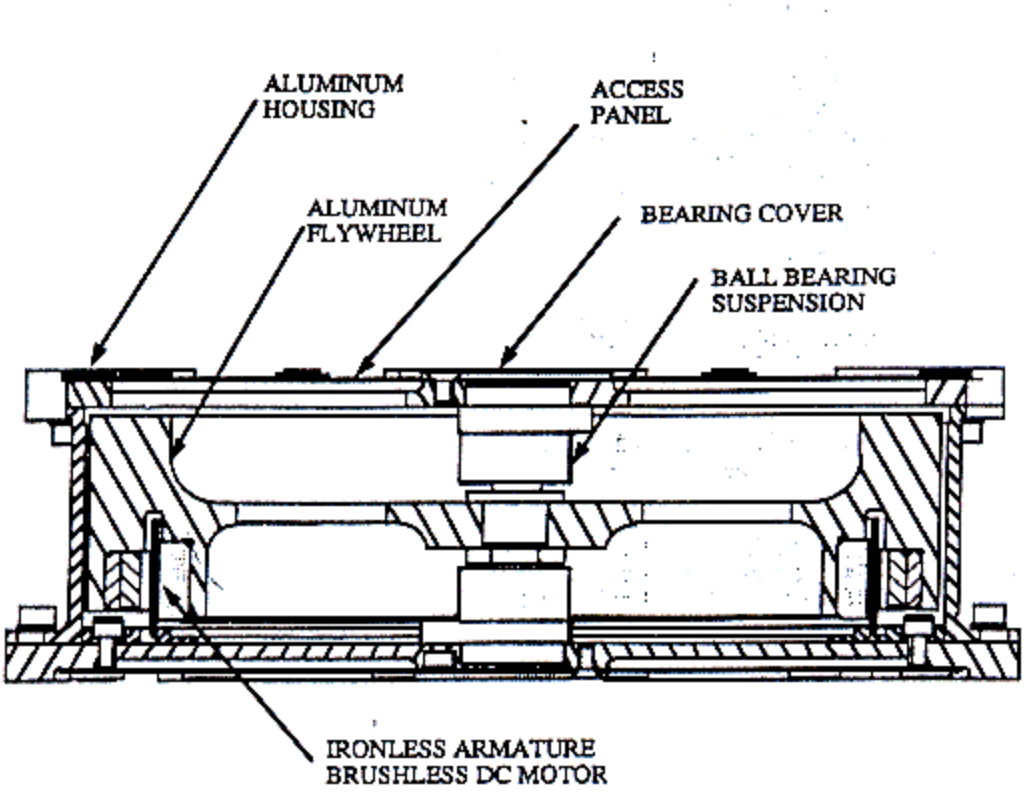

Figure 1-1: Reaction wheel cross section.

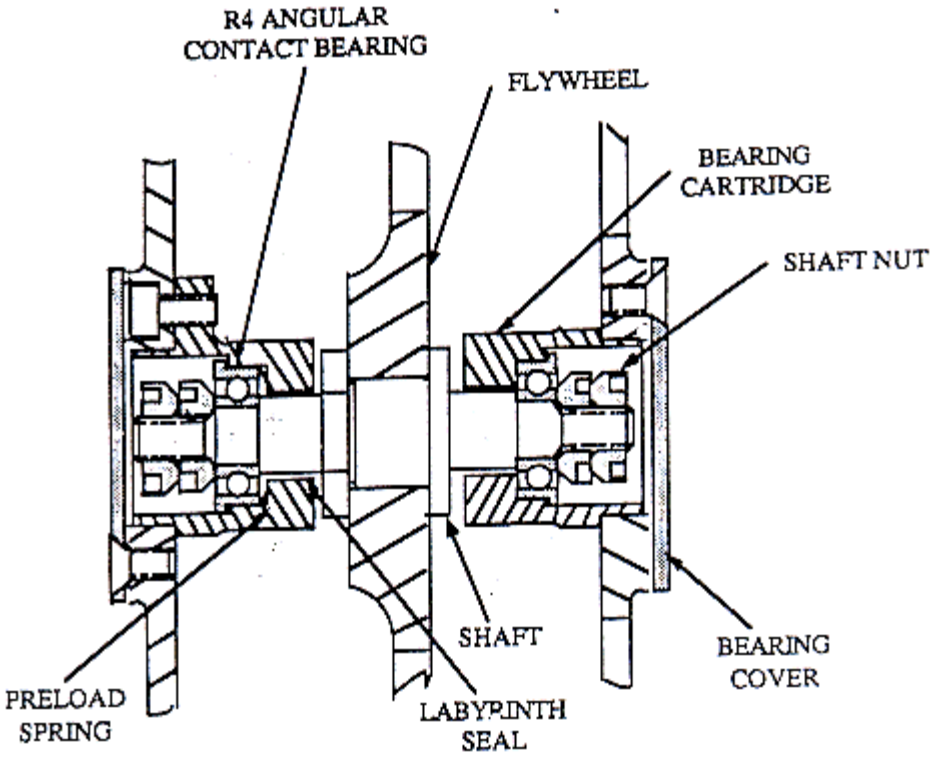

Figure 1-2: Close up of rotor shaft and mechanical assembly.

2. Requirements

2.1 Power

2.2 Size

2.3 Cost

2.4 Reliability

2.5 Angular Moment

The upper estimate of the disturbance torques are given in Table 2-1. The torque due to the magnetic field is not computed as the residual dipole moment of the satellite is not known at this time. However, this torque can be significant.

Disturbance	Symbol	Torque [Nm]	Type
Gravity Gradient	T_g	$<8.1 \times 10^{-6}$	
Aerodynamic drag	T_a	$<1.0 \times 10^{-4}$	
Solar Pressure	T_{sp}	$<7.3 \times 10^{-7}$	
Magnetic field	T_m		

Table 2-1: Disturbance torques assuming an altitude of 400 km and an inclination of 51.6^o

Modelling the satellite as a cylinder with a diameter of 0.5 m, a height of 0.5 m, and a uniform mass distribution, the moment of inertia around the x-axis will be:

$$I_{xx} = \frac{m}{4}\left(r^2 + h^2\right) = \frac{68}{4}\left(0.25^2 + 0.5^2\right) = 10.625 kg \cdot m^2$$

A pass over Tucson takes about 5 minutes. Assuming a sweep of 180^o, an angular velocity of

$$\omega = \frac{\pi}{5 \cdot 60} = 0.0175 rad/s$$

will be required. The change in angular moment for such a pass over is thus:

$$H = \omega I = 0.0175 \cdot 10.625 = 0.19 Nms$$

2.6 Torque

2.7 Environmental Requirements

3. Descriptions/Designs/Discussion

3.1 Design Specifications

Parameter	Minimum Requirement	Goal
Nominal operating speed	2000 RPM (5000 RPM max)	
Operating life	1 year	
Storage life		
Torque capability	0.02 Nm	
Torque ripple	None	<10 %
Angular momentum	0.5 Nms max	
Power consumption	< 1 W	
Weight		
Operating temperature range	$0 – 50^oC$	
Survival temperature range	$-20 – 70^oC$	
Charged particle radiation	no requirement	
Bus voltage	28 V	28 V
Size	OD 10 – 20 cm, h = 5 – 10 cm	

3.2 Structure

3.2.1 Housing

The functions of the housing are: (1) sealing the bearings; (2) structural support for rotor; (3) conductive heat sink for heat rejection from motor and bearings and (4) provide a means for mounting the assembly.

3.2.1.1 Form

The housing will be a *Pill Box Housing* and the bearings will have the inner race rotating. The advantages are: (1) easy to mount; (2) small bearings resulting in low friction. The disadvantage is a lower rocking stiffness.

3.2.1.2 Material

Aluminum (alloy 6061) will be used as principal structural material because of (1) relative low cost; (2) high thermal conductivity; (3) low stiffness. This aluminum alloy is qualified for space shuttle as listed in table 1 of MSFC-SPEC-522A.

3.2.1.3 Structural Dynamics

The stiffness of the housing is a critical structural design parameter. The structural dynamics are a function of this stiffness and the rotor mass.

If the natural frequency is too high, random vibration response accelerations will cause excessive loads to be transmitted through the bearings. If the natural frequency is too low, the frequency may fall within the range of rotation frequency during operation. Amplification of induced vibration will cause disturbances. The structural frequency should be chosen compatible with the Space Shuttle vibration data.

A lumped mass dynamic model of the reaction wheel is given in Figure 3-1.

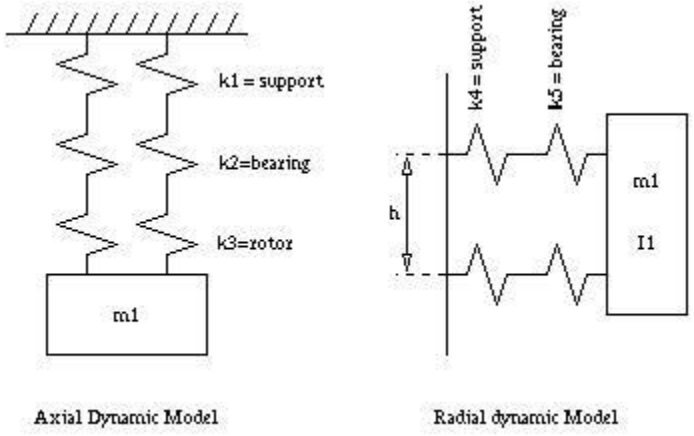

Figure 3-1: Lumped mass dynamic model of reaction wheel.

A spoked 'spider web' flexure with 6 spokes will be used to tune the structural stiffness. Effectively, changing the size of the spokes changes stiffnesses k_1 and k_4 of the model shown in Figure 3-1. A spoked flexure will also allow visual and mechanical access to the flywheel when it is completely assembled into the housing.

3.2.1.4 Sealing

The reaction wheels will be a so called *vented design*. Thin aluminum sheet is used as dust covers over the spoked support structure. Venting is achieved by a check valve effect of the cover edges. The draw back is that a vacuum jar is needed for taking test data.

3.2.2 Rotor Construction

The shaft will be made of 15-5 PH stainless steel \ to match the CTE of the bearing material as closely as practical. The hub and rim will be combined into one part which will be called flywheel. The flywheel will be made of aluminum (alloy 6061). The shaft is thermal fitted into the aluminum flywheel and secured additionally with a stainless steel hex nut.

The motor consists of high inertia cold rolled steel components bonded into the aluminum rim with structural epoxy. Samarium Cobalt magnets are bonded to the cold rolled steel ring with the same structural epoxy. Aluminum spacers are bonded in the area between the magnets for increased inertia and improved structural strength. The cold rolled steel components are plated with electroless nickel to prevent corrosion. No thermal fit on motor components to avoid thermal stresses.

Balancing is performed by removing material from the edge of the aluminum rim on a grinder. This should be sub-contracted.

3.2.3 Bearing Mounts

The selection considerations for the bearing mounts are: (1) alignment; (2) thermal compatibility and (3) prevention of fretting corrosion between similar materials.

The 15-5 PH stainless steel \ bearing mount will be aligned within the linebored housing with a precision slip fit so that the CTE is close to the CTE of the bearing material. The sleeve within the mount in which the outer race of the bearing is installed, is coated with Titanium Nitride to prevent fretting corrosion (axial movement!).

The design will be a *Spring loaded design*. One bearing is fixed while the other bearing can float axially. This assures that the bearing can move during changes in shaft and housing dimensions due to thermal expansion. The floating bearing is preloaded by a spring between the mount and the bearing.

The inner races of the bearings are secured to shaft with precision spanner nuts. A double nut scheme is used for positive locking. The second nut can be staked with epoxy since it is far enough removed from critical bearing surfaces.

3.3 Bearings

3.3.1 Type

Due to the precision and size of the bearings required for the reaction wheel, series R instrument bearings shall be used. There are two different types of series R bearings to be considered, deep groove bearings and angular contact bearings.

The deep groove bearings have full shoulders on both sides of the raceways on the inner and outer rings, while the angular contact bearings have one ring shoulder

partially or totally removed. The advantage of the deep grove bearings is that they can support radial loads, thrust loads, and combinations of loads. Angular contact bearings are capable of supporting thrust loads in one direction and combinations of radial and thrust loads, but not purely radial loads. Though the angular contact bearings are more restrictive in how they are loaded, they do have larger load and speed capacities, due to the higher ball compliment. The removed shoulder of the angular contact bearings also allow for the use of phenolic retainers as opposed to the two-piece steel ribbon type retainers required by the deep groove bearings. Phenolic retainers are advantageous due to lower retainer wear and capability of vacuum impregnating the retainer with a small supply of lubricant.

Both types of bearings can be arranged in duplex pairs, which increases capacity and rigidity, but would be more costly due to higher bearing count and the expense of matching the duplex pairs.

A set of two angular contact bearings was selected because it has low run out due to the required preload, low cost and low drag torque due to the low bearing count, and high capacity due to the angular contact bearings.

3.3.2 Preload

The series R contact bearings selected for the ball bearing suspension system require preloading. Preloading removes radial and axial play by increasing stiffness in order to allow more precise shaft positioning. Increased wear and higher drag torques are the only disadvantages of preloading.

Springs are the simplest method of preloading. They allow for thermal expansion and can tolerate a small misalignment better than alternative methods. A stainless steel wavy washer spring was selected for preloading.

3.3.3 Material

The ball bearings will be made from 440C stainless steel. This material was selected due its common use in spaceflight ball bearings and its good corrosion resistance. A more exotic material was not chosen due to the short lifetime of the spacecraft.

3.3.4 Load Ratings

The maximum loads on the bearings will occur during launch due to random vibration. To prevent plastic deformation of the bearing races, the contact stress levels must kept below 580,000 psi.

3.3.5 Tolerances

ABEC 7 class bearings or better will be used based on recommendations in DOD-A-83577A, the military specification for moving mechanical assemblies for space vehicles.

3.3.6 Selection

In order to minimize cost, bearings will be purchased *off-the-shelf* from leading bearing manufacturers. A high capacity R4 bearing from The Barden Corporation has been selected. Due to their high capacities, the Barden bearings can be used with almost any current launch vehicle random vibration spectrum. The specifications are

given in Table 3-2.

Manufacturer	Barden
Part Number	SFR4HX1
Material	440C Stainless Steel
Ball Size	9/64”
Ball Compliment	8
Contact Angle	12.7^{o}
Axial Capacity	407 lbf
Radial Capacity	206 lbf
Dynamic Load Rating	520 lbf
Maximum PSD at 365 Hz	0.26 g^2/Hz
Maximum PSD at 90 Hz	2.4 g^2/Hz
Maximum Random rms acceleration	45.2 Grms
Maximum Steady State acceleration	116 g’s

Table 3-2: Specification of selected bearings.

3.4 Lubrication

Lubrication is required to reduce wear between the ball and the race surfaces. Lubrication most commonly comes in dry films and liquid lubricants. Dry film lubricants have vacuum stability and low viscous drag, but do not have proven endurance for a continuously operating device like a reaction wheel. Therefore liquid lubrication will be used.

Pennzane X2000 has been selected due to its low vapor pressure and successful performance operating in the boundary region under vacuum conditions.

3.4.1 Lubricant Wear Testing

3.4.2 Performance

Lubricant performance is a measure of the amount bearing drag torque. Bearing drag torque is a function of lubricant viscosity.

3.4.3 Life

A conservative estimate of the evaporation loss rate is [2]:

$$G = \sqrt{\frac{M}{T}}\frac{P}{17.14}$$

where G is the evaporation rate (g/cm^2s), M is molecular weight, T is absolute temperature (K), and P is the vapor pressure (torr).

3.4.4 Optical Transmission

3.4.5 Selection

The lubricant will be selected based on two main characteristics, (1) level of bearing surface wear and (2) amount of power consumed. Another selection

consideration was whether or not the lubricant had the potential of polymerizing.

3.5 Motor Design

A three phase brushless, ironless armature motor will be employed. Advantages of a three phase brushless motor are: (1) high efficiency; (2) linear torque current relation and (3) iron is placed on flywheel increasing the moment of inertia. Disadvantages are: (1) a more complex motor drivers is required. Rotor position feedback is necessary for commutation. (2) Brushless DC motors *can* have a significant torque ripple, at a frequency corresponding to the commutation rate (number of poles times number of phases times rotation rate).

A cross section of the motor is shown in Figure 3-2. A thin armature supports the windings. On one side are the permanent magnets while a flux return path is provided on the other side. Since there is no relative movement between the magnets and the iron flux return ring, no cogging or eddy current in the flux return ring will occur. There is no need for laminating these iron parts. The air gap is relative large to ensure enough clearance on both sides of the armature. Therefore the ironless motor will be more massive as larger permanent magnets are needed. However the extra weight will contribute to the inertia of the flywheel and would be needed any way to achieve the desired inertia.

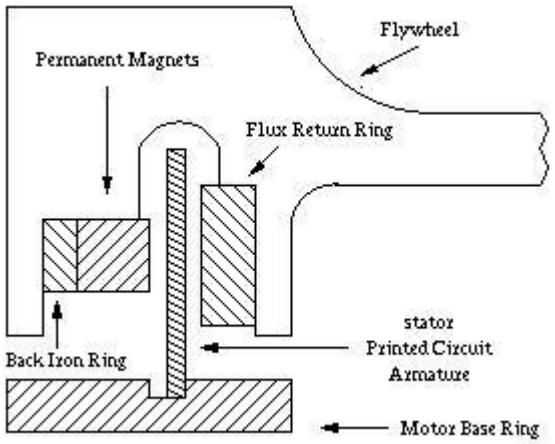

Figure 3-2: A ironless armature brushless DC motor will be integrated in the rotor.

Figure 3-3 shows a top view of the motor configuration for 36 poles. Obvious this figure is not drawn on scale. The armature is drawn thick to show all three phase windings. The final number of poles depend on the size of the permanent magnets and the radius of the motor. The back iron ring and flux return ring are made of high inertia cold rolled steel. Both rings are bonded into the aluminum rim with structural epoxy. The Samarium Cobalt permanent magnets are bonded to the cold rolled steel magnet ring with the same structural epoxy. Aluminum spacers are bonded between the magnets for increased inertia and improved structural strength. The cold rolled steel components are plated with electroless nickel to prevent corrosion. There will be no thermal fit on motor components to avoid thermal stresses.

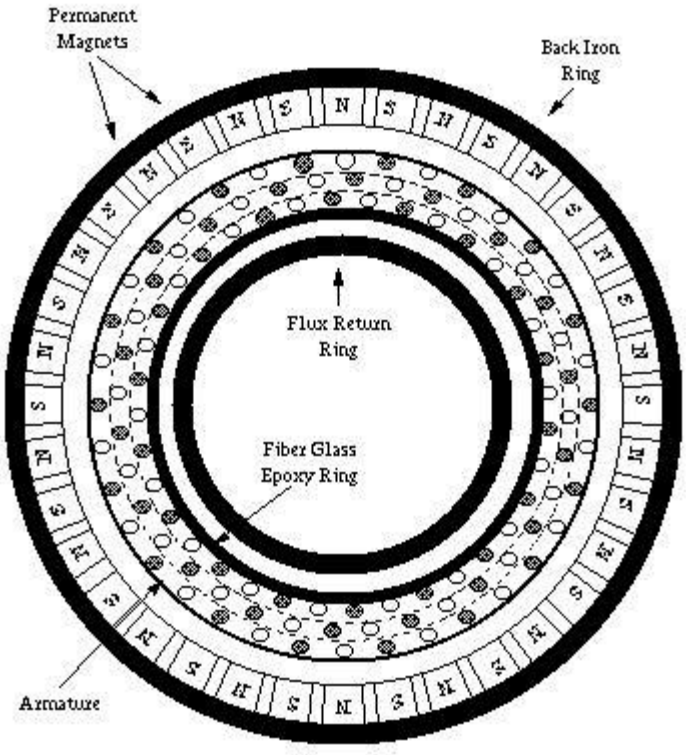

Figure 3-3: Top view of the motor configuration.

The armature consists of three flexprints, one for each phase, laminated on a fiberglass epoxy ring. The flexprints are bonded on the fiberglass epoxy ring with transfer film adhesive. Three Hall sensors are installed on the armature using transfer film adhesive.

The flexprints have a zig-zag pattern as shown in Figure 3-4. There is one zig-zag for each pole pair. The one zig-zag line shown in Figure 3-4 will be made of eight parallel conductors to reduce eddy current losses in the conductors themselves. The eight conductors will be terminated at separate pads. By changing the termination of these pads, windings can be connected all in parallel, in series parallel or all in series. This allows for changing the number of turns per pole, per phase, and thus for changing motor parameters (motor torque scale, back EMF constant). The zig-zags are separated by a distance *d*:

$$d = \frac{2\pi r}{p}$$

where *r* is the radius of the armature and *p* is the number of poles.

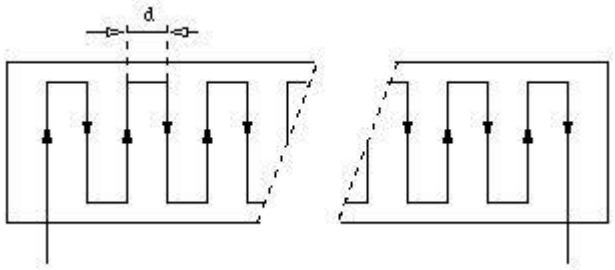

Figure 3-4: Copper pattern on flexprint for one winding.

3.6 Tachometer

A tachometer signal is required for speed and direction of rotation feedback from the reaction wheel. These signals are used by the Attitude controller. Discrete signals are needed for commutation of the brushless DC motor.

Three Hall generators will be employed for commutation of the motor. Stimulation of the Hall generators occurs directly from the permanent magnets of the motor. The resulting sinusoidal output of the sensors can easily processed into discrete commutation signals and tacho meter signals.

Hall sensors are low cost and simple. They can be integrated directly into the armature assembly.

3.7 Motor Driver

3.7.1 Design Goals

The motor has the following characteristics:

3.7.2 Motor Characteristics

The motor has the following characteristics:

Motor Type:	3 Phase brushless DC in delta connection
Position Sensors:	3 Hall sensors
Number of Poles:	36
Winding Resistance:	
Winding Inductance:	
Back EMF Constant:	

3.7.3 Driver topology

The topology of the motor driver is shown in Figure 3-5.

3.7.4 Power Bridge

As power bridge a pulse width modulated, three phase bridge will be used. For high efficiency the bridge will be constructed with power MOSFETS. Small inductors will be added in series with the windings if the winding inductance turns out to be too low.

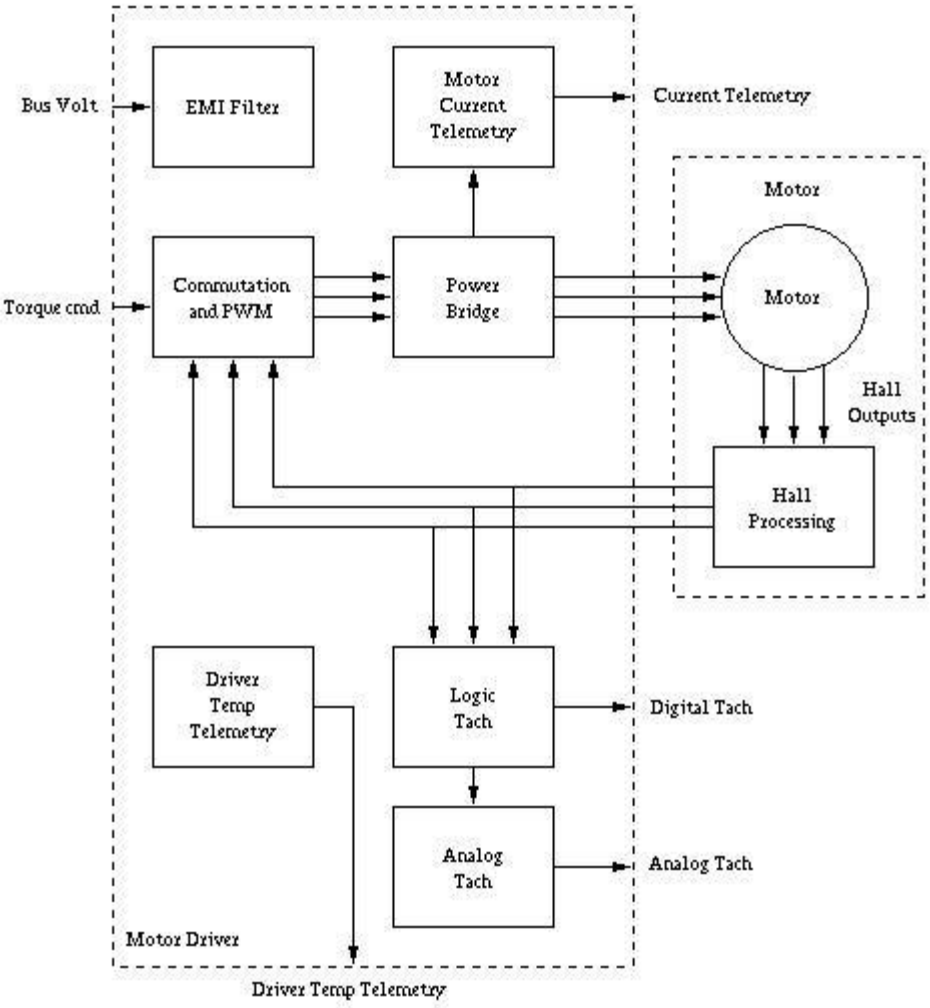

Figure 3-5: Functional block diagram of motor driver.

3.7.5 Commutation and PWM

The commutation circuitry will be build around a standard, low cost integrated circuit from Unitrode.

The IC will combine the commutation and PWM circuitry. It will be operated as 4-quadrant (voltage) drivers. This allows for reversing, delivering the kinetic energy stored in the wheel back to the power bus, and positive and negative torques.

The PWM frequency will be chosen according to the maximum electrical frequency f_e. If the wheel rotates maximum at f_r = 100 Hz (6000 RPM) than each phase signal is changing with a frequency of

$$f_e = f_r \cdot \frac{p}{2} = 100 \cdot \frac{36}{2} = 1800 Hz$$

where p is the number of poles. The PWM frequency will be chosen close to 20kHz.

3.7.6 Commands

The following commands can be send to the reaction wheel:

Driver Enable: This command will enable the driver. The driver has to be enabled before currents can be applied to the motor.

Torque Command: This analog commands determines the motor torque.

3.7.7 Telemetry Signals

The following telemetry signals will be provided:

Motor Driver Temperature: A thermistor will be located on the motor driver board to monitor the temperature. There will be no thermistor inside the wheel for monitoring the bearing temperature.

Direction of Rotation: The relative phase between two Hall sensors will be used to determine the direction of rotation.

Rotation Speed: Combining the edges from the three Hall sensors results in $3p/2$ pulses per revolution, where p is the number of poles. This digital signal will be made available. From this digital signal, an analog signal proportional to the speed will be derived and provide for attitude control.

Motor Current: An analog signal proportional to the current in the motor windings will be provided for health monitoring. It contains data about the health of the motor, bearings and motor driver.

3.7.8 Packaging

4. Lists

4.1 Mechanical Parts List

Part Number	Description	Quantity	Material
	Top support	1	Aluminum alloy 6061
	Base Support	1	Aluminum alloy 6061
	Rim	1	Aluminum alloy 6061
	Flywheel	1	Aluminum alloy 6061
	Preload spring	1	stainless steel wavy washer
	Angular contact bearings	2	
	Bearing cartridge	2	15-5 PH stainless steel
	Bearing cover	2	
	Access panel	2	Aluminum sheet
	Labyrinth seal	2	
	Shaft rotor	1	15-5 PH stainless steel
	Shaft nut	4	precision spanner

	Rotor nut Bolts	1 18	stainless steel Thread

4.2 Motor Parts List

Part Number	Description	Quantity	Material
	Flux return ring	1	
	Back iron ring	1	
	Flexprint	3	
	Epoxy armature ring	1	
	Motor base ring	1	Fiberglass epoxy
	Spacers	36	Aluminum
	Magnets	36	Samarium Cobalt

4.3 Other Items

Part Number	Description	Quantity	Material
	Structural epoxy Lubricant Transfer film adhesive		bonding and staking Pennzane X2000

5. Interface Requirements and Specifications

5.1 Physical Interface

5.2 Electrical Interface

5.3 Control Interface

6. Current Status

The current focus is to produce preliminary drawings of the reaction wheels in Pro/E. Motor selection and bearing selection are also underway. The revision of this Tech Note is also underway to reflect recent design changes.

7. Test Plan

8. Concerns and Open Issues

8.1 Reaction wheel sizing

8.2 Motor selection

8.3 Bearings selection

9. References

[1] William Bialke. *Low Cost Attitude Control System Reaction Wheel Development Final Report*. NASA-CR-191332, ITHACO, Ithaca, New York, 1991.

[2] Saul Dushman. *Scientific foundations of vacuum technique.* New York, Wiley, 1962.

[3] Peter C. Hughes. *Spacecraft attitude dynamics.* J. Wiley, 1986.

[4] Alan C. Tribble. *The space environment: implications for spacecraft design.* Princeton University Press, 1995. ISBN 0-691-03454-0.

[5] James R. Wertz, editor. *Spacecraft Attitude Determination and Control.* D. Reidel Publishing Company, 1978. ISBN 90-277-0959-9.

[6] James R. Wertz and Wiley J. Larson, editors. *Space Mission Analysis and Design*. Kluwer Academic Publishers, 1991. ISBN 0-7923-0971-5.